

REVIEW ARTICLE

## Future and advances in endoscopy

Sakib F. Elahi<sup>1</sup> and Thomas D. Wang<sup>\*,1,2</sup>

<sup>1</sup> Department of Biomedical Engineering, University of Michigan, Ann Arbor, Michigan 48109, USA

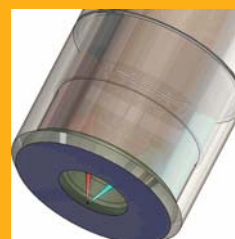
<sup>2</sup> Department of Medicine, Division of Gastroenterology, University of Michigan, 109 Zina Pitcher Pl. BSRB 1522, Ann Arbor, Michigan 48109, USA

Received 5 June 2011, revised 29 June 2011, accepted 30 June 2011

Published online 15 July 2011

**Key words:** endoscopy, wide-field, confocal, two-photon, scanning, fluorescence, molecular probes, piezoelectric

The future of endoscopy will be dictated by rapid technological advances in the development of light sources, optical fibers, and miniature scanners that will allow for images to be collected in multiple spectral regimes, with greater tissue penetration, and in three dimensions. These engineering breakthroughs will be integrated with novel molecular probes that are highly specific for unique proteins to target diseased tissues. Applications include early cancer detection by imaging molecular changes that occur before gross morphological abnormalities, personalized medicine by visualizing molecular targets specific to individual patients, and image guided therapy by localizing tumor margins and monitoring for recurrence.



Future multi-spectral dual axes confocal endomicroscope designed with MEMS mirror and piezoelectric actuator for real-time vertical cross-sectional imaging of specific molecular probes.

### 1. Introduction

Rapid technological advances promise a bright future for continued progress and innovation in endoscopy. Novel optical designs, miniature scanning mechanisms, and specific molecular probes are being developed to acquire greater biological details from tissue, including metabolic and molecular function. Instruments are being designed to provide images in various colors, more depth, and multiple dimensions that will soon be available for in vivo use. The increased variety of light sources, improved sensitivity of detectors, and availability of optical fibers are accelerating these engineering breakthroughs.

### 2. Wide-field endoscopy

Novel methods of wide-field endoscopy are critical for rapid visualization of large surface areas in hollow organs to localize disease and guide tissue biopsy. Most endoscopes use a small flexible, fiber bundle to provide illumination and a miniature video charge-coupled device (CCD) chip located in the distal tip for image detection [1]. High-resolution and a large field-of-view (FOV) can also be achieved by providing illumination with a single scanning optical fiber in the distal tip [2]. Diffraction-limited images can be achieved by using the central aperture of the objective lens. This design can achieve a much smaller in-

\* Corresponding author: e-mail: thomaswa@umich.edu, Phone: +1 (734) 936-1228, Fax: +1 (734) 647-7950

strument package, and has greater flexibility for performing multi-spectral imaging using red, green, and blue (RGB) illumination that can eventually be extended for use in molecular imaging.

### 2.1 Autofluorescence endoscopy

Early detection by routine white light endoscopy has led to a decreased incidence and mortality of cancer of the stomach and colon [3]. However, early detection remains challenging for flat and depressed lesions that have minimal morphological changes to differentiate pre-malignant from non-malignant mucosa. Over the past decade, there has been considerable effort to use differences in intrinsic fluorescence to detect pre-malignant lesions. Autofluorescence endoscopy has been developed to image endogenous fluorophores in tissue, including collagen, NADH, flavin, and porphyrins, and chromophores, such as hemoglobin, which absorbs visible light. Autofluorescence images reflect differences in the mucosal thickness, hemoglobin concentration, fluorophore distribution and concentration, and tissue microenvironment of diseased tissues. This strategy has been investigated for early detection of cancer in the lung [4], stomach [5, 6], esophagus [7, 8] and colon [9, 10], and an example of a flat colonic adenoma is shown in Figure 1b [11].

The autofluorescence imaging system (AFI, Olympus Medical Systems Corp., Tokyo, Japan), shown in Figure 1a, combines tissue autofluorescence with reflectance [11]. A xenon lamp provides illumination for autofluorescence excitation (395–475 nm) and green reflectance (540–560 nm) through a rotational filter, and two CCD detectors in the distal tip of the endoscope collect the returning light. The control unit sends the autofluorescence signal to the green channel and reflectance to the red and blue. Using this technique, normal mucosa appears as bright green autofluorescence background. Regions of in-

creased hemoglobin from ulcerated and inflamed tissue absorb green reflectance, and appear dark green. Elevated tumors have thickened mucosa and absorb the autofluorescence signal of the submucosal collagen and appear magenta, a complementary color of green [11, 12]. However, comparative studies between AFI and white light endoscopy (WLE) to detect gastric [6] and colonic [11] neoplasias suggest that although sensitivity is improved by AFI, its specificity is less than that of WLE, therefore limiting its clinical usefulness. Using wide-field fluorescence endoscopes in combination with fluorescent molecular probes can improve the specificity and clinical utility of these methodologies.

### 2.2 Scanning fiber endoscopy

The scanning fiber endoscope (SFE) uses a piezoelectric tube actuator to rapidly scan a single-mode optical fiber in a spiral pattern, as shown in Figure 2a [2]. Light from blue (440 nm), green (523 nm) and red (635 nm) lasers is delivered simultaneously through the scanning fiber, and focused by the lens assembly onto the illumination plane. The returning light is collected by a ring of multi-mode fibers located around the periphery of the housing. The image is then constructed from the full spectrum of the collected light one pixel at a time. This optical design allows for a large FOV (>100 deg) to be achieved by a very small instrument. As a result, this flexible instrument can be used to provide wide-field images of biliary and pancreatic ducts [13, 14] with ultrathin package dimensions (1.2 mm outer diameter) and with great flexibility (6 mm minimum bend radius).

The SFE was used in a pig to guide the navigation of a bronchoscope through peripheral airways for guiding tissue biopsy, as shown in Figure 2b [13]. Also, the bile duct in a pig was imaged by launching the SFE over a guide wire and through the working channel of a duodenoscope [14]. Since the RGB illu-

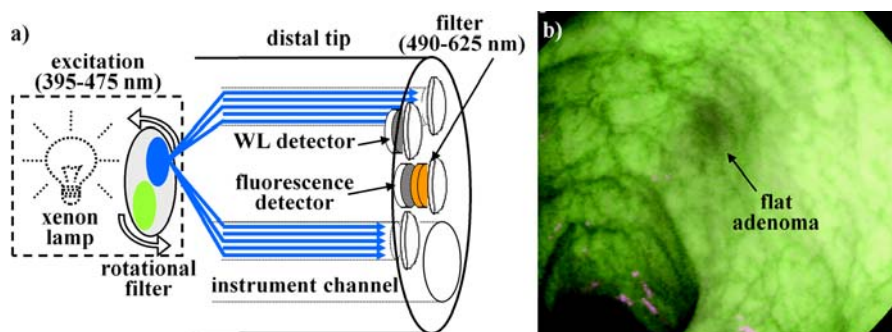


**Figure 1** (online color at: [www.biophotonics-journal.org](http://www.biophotonics-journal.org)) Autofluorescence endoscopy. (a) Illumination in 395–475 and 540–560 nm bands is generated in distal tip of endoscope by xenon lamp using a rotational filter. Autofluorescence (490–625 nm) and reflectance are collected by two CCD detectors. (b) AFI image of flat colonic adenoma. Used with permission.

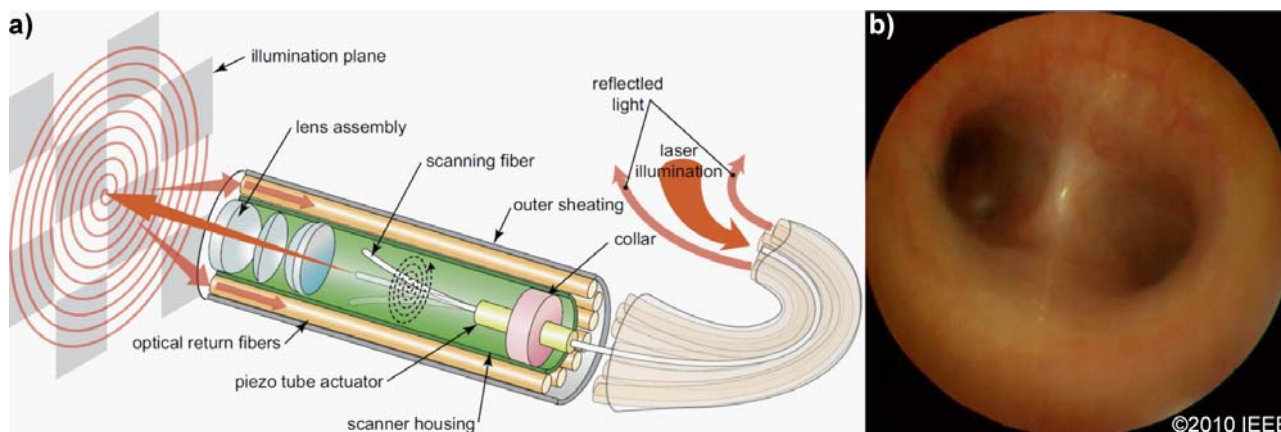


**Figure 2** (online color at: [www.biophotonics-journal.org](http://www.biophotonics-journal.org)) Scanning fiber endoscope. (a) Schematic of distal tip of scanning fiber endoscope, details in text. (b) In vivo image of peripheral airway in a pig. Used with permission.

mination sources for the SFE are narrow-band, wide-field fluorescence imaging is also possible. An exciting future direction is use of the SFE in combination with molecular probes to perform targeted imaging in hollow organs [15]. Moreover, the small size of the SFE allows for high resolution images to be collected from the esophagus, stomach, and colon of mouse models genetically engineered to express optical reporters to perform longitudinal imaging for study of molecular mechanisms of disease [16, 17]. This unique combination of spiral scanning and multi-element optics allows for this flexible fiber instrument to be realized in a miniature package to approach but not match the high-quality images of standard medical endoscopes.

### 3. Confocal and two-photon endomicroscopy

In confocal endomicroscopy, fluorescence is generated by single photons in the visible regime that excite electrons in tissue biomolecules to higher-energy levels that spontaneously relax to the ground state. The core of a single mode optical fiber acts as a spatial filter to reject scattered light that originates out of the focal plane [18]. Two-photon excited fluorescence requires two low-energy photons in the near-infrared (NIR) regime that arrive at the tissue biomolecule simultaneously and combine their energies in order to excite electrons into higher energy levels [19]. The photon flux required to generate this non-linear effect is spatially confined to a tiny focal volume. Both of these techniques perform optical sectioning to produce clear images in turbid tissue that can be used to generate 3-dimensional volumetric images.

#### 3.1 Confocal endomicroscopy

Single-photon confocal endomicroscopy systems for real-time optical biopsies have been extensively developed since the first demonstration of a fiber-optic instrument in 1993 [20]. Two endoscope-compatible confocal systems are now commercially available. One is based on a miniaturized confocal microscope (Optiscan Pty. Ltd., Victoria, Australia) that is integrated into the distal tip of a videoendoscope (EC3870K, Pentax, Tokyo, Japan) [21]. The other (Mauna Kea Technologies, Paris, France) is based on a coherent fiber bundle that can be passed down the instrument channel of most standard medical endoscopes [22]. Several groups have demonstrated high resolution imaging in hollow organs throughout the body using these instruments [23–30]. These instruments both provide horizontal cross-sectional views, in a plane parallel to the tissue surface, revealing a local view of the epithelium along a surface that tends to have a similar degree of differentiation. This orientation does not provide information about biological behavior either above or below this plane, in the basal-to-luminal direction, where cells can transform to cancer as deep as 500  $\mu\text{m}$  below the tissue surface [31]. Moreover, horizontal cross sections are an atypical view of the tissue compared to traditional H&E-stained biopsy specimens that pathologists are accustomed to viewing; hence, a trained specialist must interpret confocal endomicroscopy images.

In contrast, the dual axes architecture is a novel approach that can achieve a vertical cross-sectional view, in a plane perpendicular to the tissue surface. This innovative design employs two low numerical aperture (NA) objectives for separate illumination and collection. As a result, high resolution, long working distance, and deep tissue penetration can be achieved with an instrument package that can be

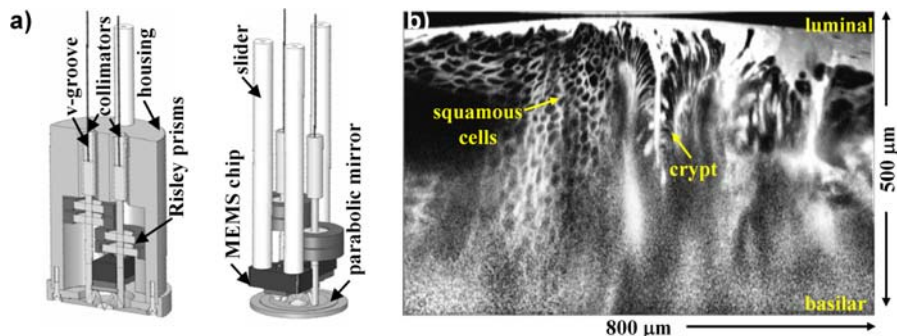


**Figure 3** (online color at: [www.biophotonics-journal.org](http://www.biophotonics-journal.org)) Dual axes confocal endomicroscopy. (a) Scanning of the overlapping beams is performed in synchrony with a gimbaled micro-mirror. (b) Vertical cross-sectional image of a neo-squamous-columnar junction in Barrett's esophagus collected with tabletop instrument over mucosal depth of 500  $\mu\text{m}$ . Used with permission.

scaled down to millimeter dimensions. In addition, post-objective scanning can provide a much larger FOV that can produce 3-dimensional (3D) volumetric images of unprecedented size [32]. The dual-axes configuration can be scaled down in size to a 5 mm diameter instrument package using a micro-electro-mechanical systems (MEMS) mirror [33], as shown in Figure 3a. The micro-mirror maintains the two beams at an angle  $\theta$  to the optical axis, and can sweep a diffraction-limited focal volume over an arbitrarily large FOV, limited only by the maximum deflection angle of the mirror. Because very little of the light that is scattered by tissue along the illumination (input) path is collected, a much higher dynamic range can be achieved. Consequently, optical sections can be collected in the vertical cross-section with NIR light to achieve deep tissue imaging, as shown in Figure 3b, acquired with a tabletop system [34]. This image was collected from the squamo-columnar junction of a patient with Barrett's esophagus. On the left half, the individual squamous cells from normal esophageal mucosa can be seen in the luminal to the basilar direction down to a depth of 500  $\mu\text{m}$ . Over the right half, vertically oriented crypts with individual mucin-secreting goblet cells associated with intestinal metaplasia can be appreciated as brightly stained vacuoles. This view shows the relationship among tissue micro-structures as they vary with depth, and provides important diagnostic information about variations in the differentiation pattern of tissue. Although MEMS scanners can be batch fabricated for mass production, the initial design and development of functional devices can require a significant investment in time and cost.

### 3.2 Two-photon endomicroscopy

Two-photon endomicroscopy offers a number of advantages over that of confocal for biological applications: 1) optical sectioning is inherent to the two-

photon process, greatly reducing tissue scattering even without need for a confocal pinhole; 2) photobleaching is significantly reduced because the high intensity excitation is confined to the small focal volume; and 3) NIR excitation penetrates deeper into the tissue [35]. The development of two-photon endomicroscopy requires the excitation to be delivered remotely to the tissue by an optical fiber that can maintain the high intensity of the light by preserving the short pulse width. Second, the size of the focusing optics must be reduced to millimeter dimensions while maintaining endoscope flexibility, achromatic properties over a broad spectral range, and high numerical aperture ( $>0.4$ ). Third, a compact scanner must sweep the focal volume over the FOV with sufficient speed to overcome motion artifact.

A two-photon endomicroscope has been developed based on the spiral piezoelectric scanner [36], shown in Figure 4a. This system uses a double-clad fiber to deliver excitation and a GRIN lens for focusing that is housed within a thin-walled hypodermic tube with outer diameter of 2.4 mm. The instrument achieves 1.6 and 11.4  $\mu\text{m}$  resolution in the lateral and axial, dimensions, respectively. A horizontal cross-sectional image of stratified squamous epithelium from rat oral mucosa stained with acridine orange at a depth of 50  $\mu\text{m}$  below the tissue surface is shown in Figure 4b. A z-stack of these images can be generated to produce the 3D volumetric image with a depth of 120  $\mu\text{m}$ , shown in Figure 4c. A limitation of two-photon endoscopy is the need for high peak powers and ultra-short pulses, resulting in expensive laser sources.

### 4. Miniature scanning and actuation mechanisms

The proximal location of the scanner has allowed for the distal end of flexible endoscopes to be ultrathin, offering the ability to access and image hollow or-

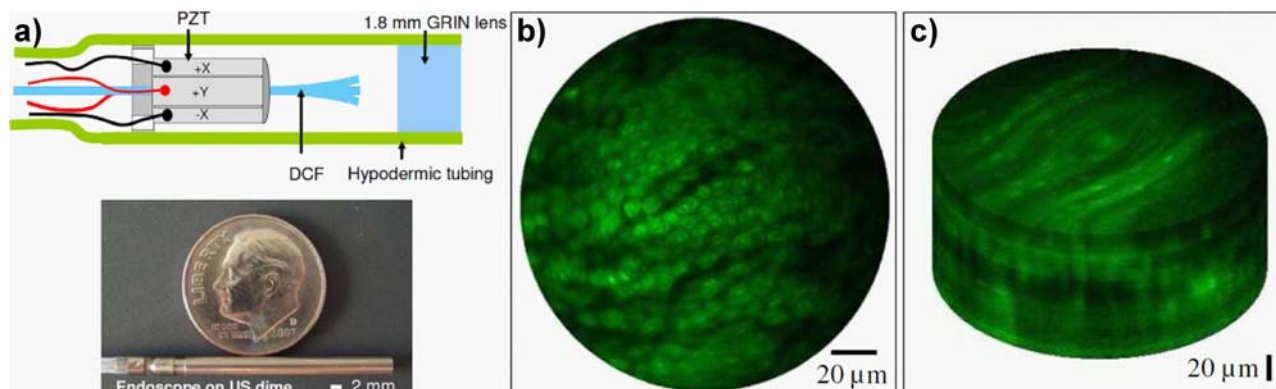


**Figure 4** (online color at: [www.biophotonics-journal.org](http://www.biophotonics-journal.org)) Two-photon endomicroscopy. (a) schematic and photo of fiber scanning instrument with dimensions of 2.4 mm. (b) Fluorescence image at 50 μm depth of rat oral mucosa stained with acridine orange. (c) 3D volumetric image with 120 μm thickness. Used with permission.

gans easily. However, the image quality is limited by pixilation artifact, and the focus cannot be adjusted for imaging at different depths. The future of wide-field and endomicroscopy imaging instruments will depend on continued progress in the development of miniature scanning and actuation mechanisms. These tiny, powerful devices spatially sweep the laser beams in the horizontal and vertical directions to rapidly generate 2D and 3D images of tissue. The performance of these mechanisms, including speed and bandwidth, determines the frame rate of the instrument, which should be at least 4 Hz to overcome motion artifact produced by organ peristalsis, heart beating, and respiratory breathing.

#### 4.1 Spiral (horizontal) scanning

Spiral scanning is performed using a central optical fiber that is cantilevered from the tip of a tubular (bulk) piezoelectric actuator, shown in Figure 5a,

and is used by the SFE [2]. The cantilever length is the extension of the fiber beyond the distal end of the tubular piezoelectric actuator, which determines the resonant frequency. By electrically driving the tube piezo near the scanning fiber's fundamental mode of lateral resonance, the fiber tip motion experiences a mechanical gain of 100 to 200 [37]. Shaping the cross-sectional axial profile along this fiber optic cantilever from a cylinder to a more complex shape by acid etching can produce additional gains of 30% to 100% [38]. Nonetheless, the general coaxial design of the SFE is ideal for the compact and simple design of ultrathin endoscopes.

This approach has been used to scan a double-clad fiber at a frequency of 1330 Hz [39] for two-photon endomicroscopy. The probe has a length of 8.2 mm and outer diameter of 2.4 mm, a package that can be easily integrated into the distal end of a medical endoscope. The piezoelectric tube is divided into four quadrants, forming two pairs of drive electrodes. The electrodes are driven with sine and cosine waveforms near resonance, 90° out of phase with

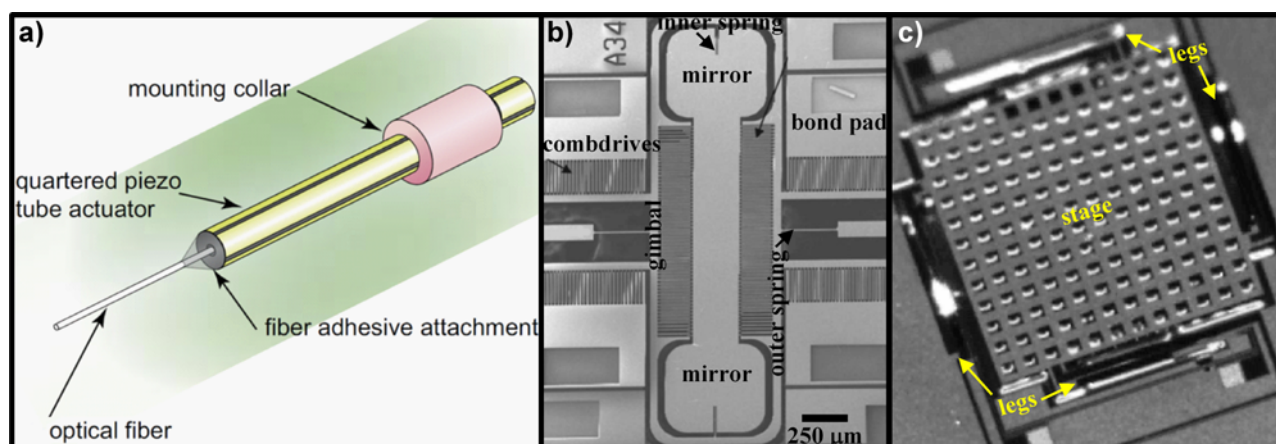


**Figure 5** (online color at: [www.biophotonics-journal.org](http://www.biophotonics-journal.org)) Miniature scanning/actuation mechanisms. (a) Spiral scanner, (b) MEMS mirror, (c) Piezoelectric z-axis actuator. Used with permission.

each other, which are then modulated with a sinusoidal waveform to achieve a spiral scan pattern. This scanner has been the core component for several two-photon endoscope configurations demonstrated in recent years [36, 39–43].

#### 4.2 MEMS (horizontal) mirrors

MEMS-based mirrors are promising for endoscopy because of their small size (0.5–2 mm diameter), high speed, low power consumption, and relatively high force output [31]. MEMS-scanners have been used in several endomicroscopes over the past decade [32, 33, 44–47]. The mirror used in the dual axes instrument is shown in Figure 5b [33]. This device has a  $600 \times 650 \mu\text{m}^2$  active mirror surface for each beam, connected together by a strut, and is designed to deflect both beams while preserving the overlapping focal volume without introducing aberrations. This micro-mirror rotates on a gimbal around an inner and outer spring in 2 dimensions. Orthogonal rows of vertical comb drives actuate the micro-mirror using electrostatic forces. The maximum optical scan angles are  $\pm 3.3^\circ$  on the inner axis and  $\pm 1.0^\circ$  on the outer axis, and the resonance frequencies of the device are 3.54 kHz and 1.1 kHz, respectively. Images can be acquired up to 30 frames per second with a maximum FOV of  $800 \times 400 \mu\text{m}^2$  using post-objective scanning. Fabrication involves 4 deep-reactive-ion etching (DRIE) steps that self-align the comb-drive fingers in the device layers. The mirror surfaces are coated with aluminum using a blanket evaporation technique to achieve  $\sim 70\%$  reflectivity at NIR wavelengths.

Two-photon endoscopes based on MEMS scanners have also been developed. A 1D scanner was demonstrated based on electrothermal biomorph actuation, is  $1 \times 1 \text{ mm}^2$  in size, has a resonance frequency of 165 Hz, and has a maximum rotation angle of  $17^\circ$  [45]. By contrast, the MEMS scanner actuated by electrostatic force had a size of  $750 \times 750 \mu\text{m}^2$ , a resonance frequency of 1.76 kHz, and a rotation angle of  $8^\circ$  [46]. A 2D MEMS scanner with dimensions  $0.5 \text{ mm} \times 0.5 \text{ mm}$  and a resonance frequency of 480 Hz has also been developed [48]. If combined with a miniature axial scanner in the future, this mirror could be used for 3D imaging of tissue. Recently, Jung and Tang et al demonstrated a 2 mm diameter MEMS scanner that achieves superior resolution, optical angle of  $14^\circ$ , and a resonance frequency of 780 Hz [49, 50].

#### 4.3 Thin film piezoelectric (vertical) actuators

Imaging with depth into the tissue requires actuators that translate the focal volume in the vertical direc-

tion. Various forms of shape memory alloys are currently used, but are limited in performance by hysteresis and slow speeds [42]. Thin-film piezoelectric materials are promising for future use in endomicroscopy to perform vertical translation. These actuators can achieve large displacements with high bandwidth using low-voltage and power levels, features that are compatible with in vivo imaging in medical endoscopes. The actuation material is a chemical-solution deposited lead–zirconate–titanate (PZT) thin film. As shown in Figure 5c, a set of 4 compound bend-up/bend-down unimorphs can be used to produce translational motion of a moving stage that seats a horizontal scanning device. Prototype designs have shown as much as  $120 \mu\text{m}$  of static displacement using 4 legs with a length of  $920 \mu\text{m}$ . The system resonance is observed at a frequency of  $\sim 200 \text{ Hz}$ . Greater vertical displacement can be achieved by stacking these legs in the vertical direction [51].

### 5. Molecular imaging

The commercialized and preclinical instruments described above have mostly been demonstrated using non-specific fluorescence contrast agents. The clinical utility of these instruments can be greatly supplemented by integrating them with molecular probes that are highly specific for disease targets. Molecular imaging allows for in vivo visualization and characterization of biological processes that occur on a cellular or sub-cellular scale based on protein expression [52]. These imaging agents are usually integrated with advanced endoscopic instruments that are sensitive to fluorescence. Applications include 1) early cancer detection by imaging molecular changes that occur before gross morphological abnormalities; 2) personalized medicine by visualizing molecular targets specific to individual patients; and 3) image guided therapy by localizing tumor margins and monitoring for recurrence [53].

#### 5.1 Classifications of molecular probes

The best molecular probes are highly specific for their biological targets, active only in the presence of disease, and much more intense than the surrounding background. For clinical use, the ideal probe should have rapid binding kinetics (time scale of minutes), be easy to label with fluorescent agents in multiple colors, and have capability for low cost, large scale synthesis [54]. The two most common classes of probes being developed for clinical use include antibodies and peptides. Antibodies are highly specific for known targets, but have been difficult to translate into the clinic because of delivery chal-

lenges, longed serum half-lives, and immunogenicity. Peptides are short chains of amino acids that have been successfully selected using phage display technologies that consist of high diversity, unbiased libraries. However, the selection process for specific peptides can be challenging. While their binding affinity is not as high as that of antibodies, peptides are much smaller in size, easy to label with fluorescent dyes, have rapid binding kinetics, and minimal immunogenicity.

Molecular probe platforms include activatable, antibody/affibody, small molecule, peptide, and aptamer, as shown in Figure 6. Activatable probes are designed to generate fluorescence only after coming into contact with the target. These “smart” probes are fluorescently quenched in their native state, and are activated when cleaved by tumor-associated proteases, such as cathepsin and matrix metalloproteinases which play an important role in cell proliferation, invasion, apoptosis, angiogenesis, and metastasis [55]. Antibodies are widely used Y-shaped gamma globulins (IgG) that bind specifically to antigenic targets. They can be labeled with a large selection of fluorescent dyes, and have been developed for several molecular targets that have great clinical relevance, including human epidermal growth factor receptor (HER2) and epidermal growth factor receptor (EGFR) [27]. Antibodies may elicit an immune reaction with repeated use, and are costly to produce in large quantities. Affibodies are small single domain proteins that are desirable because of their small size, leading to rapid tumor localization and fast clearance [56]. Their utility has been demonstrated for *in vivo* targeting and detection of tumors that over express HER2. Small molecule probes have been developed for imaging that are activated by a change in pH after entering a target cell and merging with lysosomes [57]. These probes require a targeting moiety such as HER2 antibody to attach to the cell. Since non-activated probes do not emit a signal, the target-to-background ratio is greatly improved. Aptamers are single-stranded, nuclease-resistant DNA or RNA molecules [58], and have re-

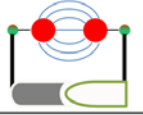
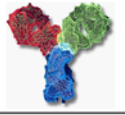
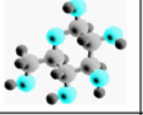
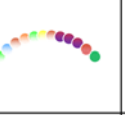
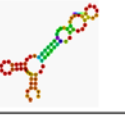
cently been developed with high affinity and specificity for DLD-1 and HCT 116 colorectal cancer cell lines *in vitro*, but this has not yet been demonstrated *in vivo*.

### 5.2 Molecular targets

Targets unique to disease can be over-expressed both on the cell-surface as well as within the cytoplasm. For purposes of imaging, the pharmacokinetics of molecular probes that bind to the cell surface are more predictable than those that are internalized and broken down by proteolytic enzymes. Epidermal growth factor receptor (EGFR), HER2/neu (ERBB2), and vascular endothelial growth factor (VEGF) receptor are over-expressed in several cancers, including esophageal, colorectal, breast, and ovarian. Somatostatin receptors (SSTR) are overexpressed in neuroendocrine tumors [59]. Over-expressed proteolytic enzymes activate “smart” probes such as cathepsin-B and matrix metalloproteinases (MMPs) [60–62]. Apoptosis reporters frequently utilizes effector caspases as targets [63].

### 5.3 *In vivo* targeted molecular imaging

Targeted molecular imaging has been demonstrated mostly in the colon thus far, using different types of probes on a variety of instrumentation platforms. A fluorescein-labeled monoclonal antibody against EGFR has been imaged using confocal laser endomicroscopy in a xenograft mouse model of colorectal cancer [27]. Image analysis indicated that fluorescence intensity was higher in tumors that have high EGFR expression than those with low EGFR expression. Clinical use of peptides was demonstrated for early detection of colorectal cancer using the FITC-labeled sequence VRPMLQ, as shown in Figure 7 [28]. The peptide bound more specifically to dysplastic colonocytes than to adjacent normal cells with 81% sensitivity and 82% specificity on confocal

	Activatable	Antibody/ Affibody	Small Molecule	Peptide	Aptamer
Molecular Probe					
Strengths	amplification ↑ target/background known targets	↑ specificity ↑ diversity ↑ affinity known targets	↓ background reversible flexible labeling	↓ size ↑ diversity ↓ immunogenicity ↓ cost	↓ size ↑ diversity ↓ immunogenicity ↑ affinity
Weaknesses	↓ signal few probes ? toxicity	immunogenicity ↑ cost ↓ quantity	variable specificity ? toxicity	↓ affinity ↓ Possible degradation	↑ cost ↓ quantity ? toxicity

**Figure 6** (online color at: [www.biophotonics-journal.org](http://www.biophotonics-journal.org)) Molecular probe platforms. Strengths and weaknesses of various probe platforms being developed for targeted imaging are presented.

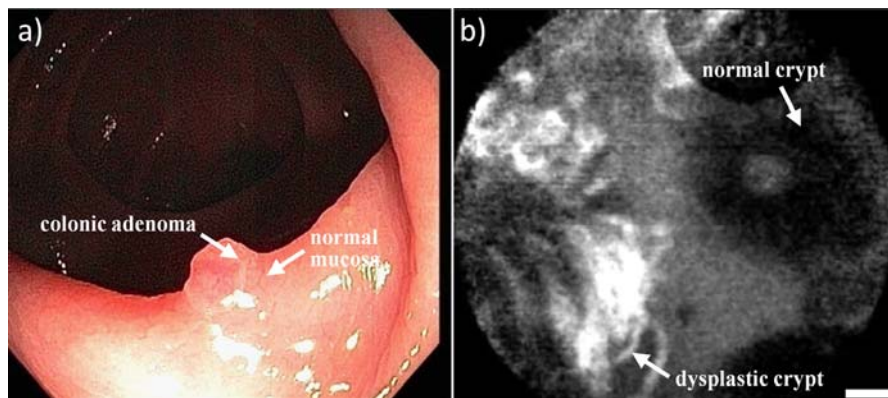


**Figure 7** (online color at: [www.biophotonics-journal.org](http://www.biophotonics-journal.org)) Targeted imaging of colonic dysplasia. In vivo confocal fluorescence images of the border between colonic adenoma and normal mucosa showing peptide binding to dysplastic colonocytes: (a) endoscopic view, (b) border on confocal endomicroscopy, scale bars: 20  $\mu\text{m}$ . Used with permission.

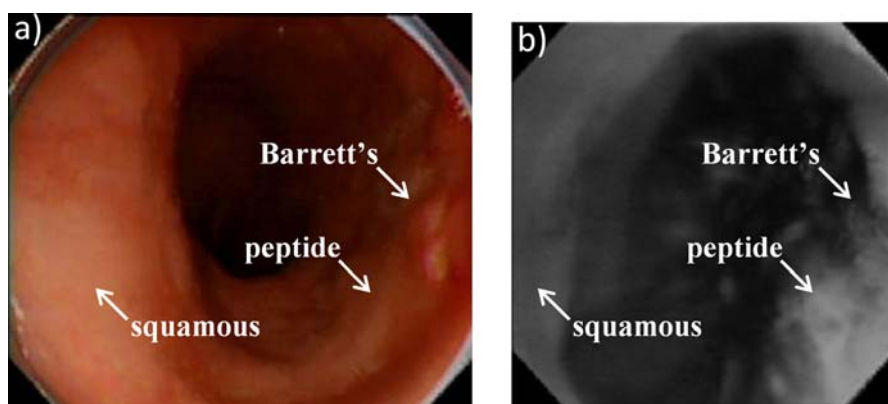


**Figure 8** (online color at: [www.biophotonics-journal.org](http://www.biophotonics-journal.org)) Targeted imaging of esophageal dysplasia. Targeted detection of high-grade dysplasia in Barrett's esophagus with fluorescence imaging. (a) White light endoscopic image of Barrett's esophagus shows absence of architectural features to guide biopsy for dysplasia. (b) Molecular image after topical administration of labeled peptides shows increased fluorescence intensity at a site (arrow) of high-grade dysplasia. Used with permission.

laser endomicroscopy. Molecular imaging has also been demonstrated for early detection of esophageal cancer. Li et al recently identified the peptide SNFYMPL that preferentially binds to high-grade dysplasia in Barrett's esophagus on excised human specimens, and plans have been made to study this peptide in a Phase 1 clinical trial [64]. Another FITC-labeled peptide, ASYNYDA, has been selected to target dysplastic esophageal mucosa, and has been demonstrated to have higher fluorescence intensity for high grade dysplasia in a pilot clinical study using the AFI endoscope, as shown in Figure 8 [53].

## 6. Conclusions

Endoscopy is a powerful imaging tool for rapidly visualizing large surface areas in hollow organs, such as the colon, esophagus, lung, oropharynx, and sto-

mach. New instruments that are sensitive to fluorescence are being developed to observe endogenous biochemical substrates associated with increased metabolism. In addition, novel optical designs are being implemented to reduce the instrument size to clearly visualize the biliary and pancreatic ducts. These hollow organs can also be studied with techniques of endomicroscopy, such as confocal and two-photon, that perform optical sectioning for looking below the tissue surface with sub-cellular resolution. These methods rely on novel scanning and actuation mechanisms based on MEMS (microelectromechanical systems) and PZT (piezoelectric) technologies.

The future of endoscopy lies in the development of new imaging technologies that allow physicians to see beyond gross anatomical structures to appreciate biological function. The molecular properties of tissue possess a significant wealth of information that reveals details about tissue behavior that can be discovered when properly imaged. Diseases such as



**Table 1.** Comparison of performance characteristics for emerging endoscopic technologies.

	Autofluorescence endoscopy [65]	Scanning fiber endoscopy [2]	Single axis confocal endomicroscopy*	Dual axes confocal endomicroscopy [31]	Spiral-scanning 2-photon endomicroscopy [36]	MEMS-based 2-photon endomicroscopy [49]
Diameter (mm)	11	1.2	12.8	5.5	2.4	2
Lateral Res ( $\mu\text{m}$ )	<1000	<1000	0.7	5.5	1.6	2
Axial Res ( $\mu\text{m}$ )	N/A	N/A	7	7.5	11.4	10
Field of view	140°	100°	400 $\mu\text{m}$	800 $\times$ 500 $\mu\text{m}$	320 $\mu\text{m}$	200 $\mu\text{m}$
Frame rate (Hz)	30	30	0.8	2	3.3	0.25
Penetration depth ( $\mu\text{m}$ )	0	0	0–250	0–500	120	210
Stage of development	Clinical	Clinical	Clinical FDA approved	Clinical	Pre-clinical	Pre-clinical

\* Parameters listed for Optiscan/Pentax system [21].

cancer result from a number and variety of genetic changes. Thus, the in vivo molecular expression patterns of cells and tissues can provide physicians with information on how to improve patient management. Confocal and two-photon endomicroscopy are exciting new techniques that perform optical sectioning in real time to visualize tissue with sub-cellular details to provide “in situ histology”. The images are being created using advancements in miniature scanning mechanisms that operate with high speeds needed to overcome motion artifact. Progress is also being made in methods for performing wide-area imaging that enable observation of large mucosal surfaces to localize the presence of disease.

**Acknowledgements** This work was funded by NIH (U54 CA136429, P50 CA93990, and R01 CA142750). The authors thank Zhongyao Liu and Zhen Qiu for the abstract picture.

**Conflict of interest** Parts of this manuscript describe intellectual property filed on behalf of author TD Wang by the University of Michigan.



**Sakib Elahi** received a B.S. in Mech Eng in 2006 and M.S.E. in Biomed Eng in 2008 from the University of Michigan. He participated in the R&D Design Engineering Co-op at Ethicon Endo-Surgery, Inc. where he designed and prototyped ultrasonic cutting/coagulating surgical devices. He is currently a Ph.D. student in the Department of Biomed Eng at the University of Michigan in Professor Wang’s laboratory. In 2010, he won first place in the Technical Session Competition for Engineering in Medical Systems at University of Michigan Engineering Graduate Symposium.



**Thomas D. Wang** received a B.S. in Physics from Harvey Mudd College in 1985, Ph.D. in Biomedical Eng from MIT in 1996, and M.D. from Harvard Medical School in 1998. He is an Associate Prof of Medicine and BME and P.I. of the Network for Translational Research (<http://sitemaker.umich.edu/ntr>) at the University of Michigan. In addition,

Dr. Wang is a board-certified gastroenterologist who has pioneered the development of wide-area fluorescence endoscopy, the dual axes confocal microscope, and clinical use of fluorescence-labeled peptides to detect dysplasia in the gastrointestinal tract.

## References

- [1] T. George and W. Thomas, in: G. Zouridakis and J. Moore (eds.), *Biomedical Technology and Devices Handbook* (CRC Press, 2004).
- [2] C. M. Lee, C. J. Engelbrecht, T. D. Soper, F. Helmchen, and E. J. Seibel, *J. Biophotonics* **3**, 385–407 (2010).
- [3] A. Jemal, R. Siegel, J. Xu, and E. Ward, *CA Cancer J. Clin.* **60**, 277–300 (2010).
- [4] E. Edell, S. Lam, H. Pass, Y. E. Miller, T. Sutedja, T. Kennedy, G. Loewen, R. L. Keith, and A. Gazdar, *J. Thorac. Oncol.* **4**, 49–54 (2009).
- [5] A. Ohkawa, H. Miwa, A. Namihisa, O. Kobayashi, N. Nakaniwa, T. Ohkusa, T. Ogihara, and N. Sato, *Endoscopy* **36**, 515–521 (2004).
- [6] M. Kato, M. Kaise, J. Yonezawa, Y. Yoshida, and H. Tajiri, *Endoscopy* **39**, 937 (2007).
- [7] M. Kara, F. Peters, F. Tenkate, S. Vandeventer, P. Fockens, and J. Bergman, *Gastrointest. Endosc.* **61**, 679 (2005).

- [8] M. A. Kara, F. P. Peters, P. Fockens, F. J. ten Kate, and J. J. Bergman, *Gastrointest. Endosc.* **64**, 176–185 (2006).
- [9] T. Matsuda, Y. Saito, K. Fu, T. Uraoka, N. Kobayashi, T. Nakajima, H. Ikehara, Y. Mashimo, T. Shimoda, Y. Murakami, A. Parra-Blanco, T. Fujimori, and D. Saito, *Am. J. Gastroenterol.* **103**, 1926 (2008).
- [10] A. L. McCallum, J. T. Jenkins, D. Gillen, and R. G. Molloy, *Gastrointest. Endosc.* **68**, 283–290 (2008).
- [11] N. Uedo, K. Higashino, R. Ishihara, Y. Takeuchi, and H. Iishi, *Digestive Endoscopy* **19**, S134 (2007).
- [12] M. Kato, N. Uedo, R. Ishihara, T. Kizu, R. Chatani, T. Inoue, E. Masuda, K. Tatsumi, Y. Takeuchi, K. Higashino, H. Iishi, Y. Tomita, and M. Tatsuta, *Gastric Cancer* **12**, 219–224 (2009).
- [13] T. D. Soper, D. R. Haynor, R. W. Glenny, and E. J. Seibel, *IEEE Trans. Biomed. Eng.* **57**, 736–745 (2010).
- [14] E. J. Seibel, C. M. Brown, J. A. Dornitz, and M. B. Kimmey, *Gastrointest. Endosc. Clin. N. Am.* **18**, 467–78, viii (2008).
- [15] S. J. Miller, C. M. Lee, B. P. Joshi, E. J. Seibel, and T. D. Wang, *Gastroenterology* **140**, S-11 (2011).
- [16] S. J. Miller, B. P. Joshi, Y. Feng, A. Gaustad, E. R. Fearon, and T. D. Wang, *PLoS One* **6**, e17384 (2011).
- [17] S. F. Elahi, S. J. Miller, B. Joshi, and T. D. Wang, *Biomed. Opt. Express* **2**, 981–986 (2011).
- [18] J. B. Pawley, *Handbook of Biological Confocal Microscopy* (Springer Science+Business Media, New York City, 2006).
- [19] W. Denk, J. H. Strickler, and W. W. Webb, *Science* **248**, 73–76 (1990).
- [20] A. F. Gmitro and D. Aziz, *Opt. Lett.* **18**, 565 (1993).
- [21] R. Kiesslich, J. Burg, M. Vieth, J. Gnaendiger, M. Enders, P. Delaney, A. Polglase, W. McLaren, D. Janell, S. Thomas, B. Nafe, P. R. Galle, and M. F. Neurath, *Gastroenterology* **127**, 706–713 (2004).
- [22] T. D. Wang, S. Friedland, P. Sahbaie, R. Soetikno, P. L. Hsiung, J. T. Liu, J. M. Crawford, and C. H. Contag, *Clin. Gastroenterol. Hepatol.* **5**, 1300–1305 (2007).
- [23] R. Kiesslich, L. Gossner, M. Goetz, A. Dahlmann, M. Vieth, M. Stolte, A. Hoffman, M. Jung, B. Nafe, P. R. Galle, and M. F. Neurath, *Clin. Gastroenterol. Hepatol.* **4**, 979–987 (2006).
- [24] A. L. Polglase, W. J. McLaren, S. A. Skinner, R. Kiesslich, M. F. Neurath, and P. M. Delaney, *Gastrointest. Endosc.* **62**, 686–695 (2005).
- [25] A. L. Polglase, W. J. McLaren, and P. M. Delaney, *Expert Rev. Med. Devices* **3**, 549–556 (2006).
- [26] E. M. Bott, I. R. Young, G. Jenkin, and W. J. McLaren, *Am. J. Obstet. Gynecol.* **194**, 105–112 (2006).
- [27] M. Goetz, A. Ziebart, S. Foersch, M. Vieth, M. J. Waldner, P. Delaney, P. R. Galle, M. F. Neurath, and R. Kiesslich, *Gastroenterology* **138**, 435–446 (2010).
- [28] P. L. Hsiung, J. Hardy, S. Friedland, R. Soetikno, C. B. Du, A. P. Wu, P. Sahbaie, J. M. Crawford, A. W. Lowe, C. H. Contag, and T. D. Wang, *Nat. Med.* **14**, 454–458 (2008).
- [29] G. A. Sonn, K. E. Mach, K. Jensen, P. L. Hsiung, S. N. Jones, C. H. Contag, T. D. Wang, and J. C. Liao, *J. Endourol.* **23**, 197–201 (2009).
- [30] H. Pohl, T. Rosch, M. Vieth, M. Koch, V. Becker, M. Anders, A. C. Khalifa, and A. Meining, *Gut* **57**, 1648–1653 (2008).
- [31] W. Piyawattanametha and T. D. Wang, in: Tunnell J (ed.), *Microendoscopy: In Vivo Clinical Imaging and Diagnosis* (McGraw Hill Professional, New York, NY, 2011).
- [32] T. D. Wang, M. J. Mandella, C. H. Contag, and G. S. Kino, *Opt. Lett.* **28**, 414–416 (2003).
- [33] J. T. Liu, M. J. Mandella, H. Ra, L. K. Wong, O. Solgaard, G. S. Kino, W. Piyawattanametha, C. H. Contag, and T. D. Wang, *Opt. Lett.* **32**, 256–258 (2007).
- [34] J. T. Liu, M. J. Mandella, J. M. Crawford, C. H. Contag, T. D. Wang, and G. S. Kino, *J. Biomed. Opt.* **13**, 034020 (2008).
- [35] F. Helmchen and W. Denk, *Nat. Methods* **2**, 932–940 (2005).
- [36] Y. Wu, Y. Leng, J. Xi, and X. Li, *Opt. Express* **17**, 7907–7915 (2009).
- [37] Q. Y. J. Smithwick, P. G. Reinhall, J. Vagners, and E. J. Seibel, *J. Dyn. Syst. Meas. Control* **126**, 88 (2004).
- [38] C. M. Brown, P. G. Reinhall, S. Karasawa, and E. J. Seibel, *Opt. Eng.* **45**, 043001 (2006).
- [39] M. T. Myaing, D. J. MacDonald, and X. Li, *Opt. Lett.* **31**, 1076–1078 (2006).
- [40] C. J. Engelbrecht, R. S. Johnston, E. J. Seibel, and F. Helmchen, *Opt. Express* **16**, 5556–5564 (2008).
- [41] Y. Wu, J. Xi, M. J. Cobb, and X. Li, *Opt. Lett.* **34**, 953–955 (2009).
- [42] Y. Wu, Y. Zhang, J. Xi, M. J. Li, and X. Li, *J. Biomed. Opt.* **15**, 060506 (2010).
- [43] K. Murari, Y. Zhang, S. Li, Y. Chen, M. J. Li, and X. Li, *Opt. Lett.* **36**, 1299–1301 (2011).
- [44] W. Piyawattanametha, R. P. Barretto, T. H. Ko, B. A. Flusberg, E. D. Cocker, H. Ra, D. Lee, O. Solgaard, and M. J. Schnitzer, *Opt. Lett.* **31**, 2018–2020 (2006).
- [45] L. Fu, A. Jain, H. Xie, C. Cranfield, and M. Gu, *Opt. Express* **14**, 1027–1032 (2006).
- [46] C. L. Hoy, N. J. Durr, P. Chen, W. Piyawattanametha, H. Ra, O. Solgaard, and A. Ben-Yakar, *Opt. Express* **16**, 9996–10005 (2008).
- [47] H. Ra, W. Piyawattanametha, M. J. Mandella, P. L. Hsiung, J. Hardy, T. D. Wang, C. H. Contag, G. S. Kino, and O. Solgaard, *Opt. Express* **16**, 7224–7232 (2008).
- [48] L. Fu, A. Jain, C. Cranfield, H. Xie, and M. Gu, *J. Biomed. Opt.* **12**, 040501 (2007).
- [49] S. Tang, W. Jung, D. McCormick, T. Xie, J. Su, Y. C. Ahn, B. J. Tromberg, and Z. Chen, *J. Biomed. Opt.* **14**, 034005 (2009).
- [50] W. Jung, S. Tang, D. T. McCormick, T. Xie, Y. C. Ahn, J. Su, I. V. Tomov, T. B. Krasieva, B. J. Tromberg, and Z. Chen, *Opt. Lett.* **33**, 1324–1326 (2008).
- [51] Z. Qiu, J. S. Pulskamp, X. Lin, C. Rhee, T. Wang, R. G. Polcawich, and K. Oldham, *J. Micromech. Microengineering* **20**, 075016 (2010).
- [52] R. Weissleder, *Science* **312**, 1168 (2006).
- [53] M. Goetz and T. D. Wang, *Gastroenterology* **138**, 828–33.e1 (2010).
- [54] M. Li and T. D. Wang, *Gastrointest. Endosc. Clin. N. Am.* **19**, 283–298 (2009).

- [55] U. Mahmood, *Mol. Cancer Ther.* **2**, 489 (2003).
- [56] V. Tolmachev, A. Orlova, F. Y. Nilsson, J. Feldwisch, A. Wennborg, and L. Abrahmsen, *Expert Opin. Biol. Ther.* **7**, 555–568 (2007).
- [57] Y. Urano, D. Asanuma, Y. Hama, Y. Koyama, T. Barrett, M. Kamiya, T. Nagano, T. Watanabe, A. Hasegawa, P. L. Choyke, and H. Kobayashi, *Nat. Med.* **15**, 104–109 (2009).
- [58] K. Sefah, L. Meng, D. Lopez-Colon, E. Jimenez, C. Liu, and W. Tan, *PLoS One* **5**, e14269 (2010).
- [59] K. E. Oberg, J. C. Reubi, D. J. Kwakkeboom, and E. P. Krenning, *Gastroenterology* **139**, 742–53, 753.e1 (2010).
- [60] C. H. Tung, U. Mahmood, S. Bredow, and R. Weissleder, *Cancer Res.* **60**, 4953–4958 (2000).
- [61] A. Faust, B. Waschkau, J. Waldeck, C. Holtke, H. J. Breyholz, S. Wagner, K. Kopka, W. Heindel, M. Schafers, and C. Bremer, *Bioconjug. Chem.* **19**, 1001–1008 (2008).
- [62] C. Bremer, S. Bredow, U. Mahmood, R. Weissleder, and C. H. Tung, *Radiology* **221**, 523–529 (2001).
- [63] K. E. Bullock, D. Maxwell, A. H. Kesarwala, S. Gammon, J. L. Prior, M. Snow, S. Stanley, and D. Piwnicka-Worms, *Biochemistry-US* **46**, 4055–4065 (2007).
- [64] M. Li, C. P. Anastassiades, B. Joshi, C. M. Komarck, C. Piraka, B. J. Elmunzer, D. K. Turgeon, T. D. Johnson, H. Appelman, D. G. Beer, and T. D. Wang, *Gastroenterology* **139**, 1472–1480 (2010).
- [65] N. Uedo, H. Iishi, R. Ishihara, K. Higashino, and Y. Takeuchi, *Digestive Endoscopy* **18**, S131 (2006).